Magnetization Reversal Process in L10-FePt(001)Dot Arrays (L10-FePt(001)ドット配列の磁化反転過程)

著者	王 東玲
号	53
学位授与番号	4044
URL	http://hdl.handle.net/10097/42458

氏名	わんどんりん 王 東 玲
授与学位	博士（工学）
学位授与年月日	平成２０年９月１１日
学位授与の根拠法規	学位規則第４条第１項
研究科，専攻の名称	東北大学大学院工学研究科（博士課程）知能ﾃﾞﾊﾞｲｽ材料学 専攻
学位論文題目	Magnetization Reversal Process in $L1_0$-FePt (001) Dot Arrays ($L1_0$-FePt(001)ドット配列の磁化反転過程)
指導教員	東北大学教授 高梨 弘毅
論文審査委員	主査 東北大学教授 高梨 弘毅 東北大学教授 杉本 諭 東北大学教授 北上 修

論文内容要旨

1. Background

Magnetic nanostructured materials have attracted a great deal of attention, because of novel and enhanced properties over their counterparts. The demand for ultrahigh density magnetic storage devices drives the bit size into nanometer scale and $L1_0$ ordered FePt alloy with a huge uniaxial magnetic anisotropy (K_u = 7×10^7erg/cc) is one of the most promising candidate materials for future ultrahigh density magnetic recording media, such as patterned media. Magnetization reversal which determines the coercive field in different types of permanent magnets, is one important issue for magnetic nanostructured materials. A phenomenological analysis, proposed from the viewpoint of the inhomogeneity of nanostructure, has been applied to a wide range of magnets. However, such a phenomenological analysis technique has not been used to understand the magnetization reversal process of $L1_0$-FePt ordered alloys.

This study focuses on the magnetization reversal process in microfabricated $L1_0$-FePt (001) dot arrays with well-defined geometry, which are suitable for the precise analysis of the magnetization process in reduced dimensions. The main objective of this study is to understand the magnetization reversal process in $L1_0$-FePt (001) dots by the phenomenological analysis. First, the magnetization reversal process is investigated and the defect region is evaluated in $L1_0$-FePt (001) circular dots with diameter (d) of 0.25 μm. Next, the dot size dependence of magnetization reversal process is analyzed for d = 0.16, 0.25, 1, 2.3 and 5 μm. Furthermore, the magnetization reversal process in $L1_0$-FePt (001) particulate films is investigated and compared with the results of $L1_0$-FePt (001) dots. Finally, micromagnetic simulations are performed taking into account structural inhomogeneity and the simulated results are compared with the experimental results.

2. Experimental

$L1_0$-FePt (001) continuous films were prepared on MgO (001) substracts using an ultra high vacuum magnetron sputtering system. A 1 nm-thick Fe seed layer and a 40 nm-thick Au buffer layer were first deposited at room temperature. Then, a 50 nm-thick FePt (001) layer was epitaxially grown at 300°C, and subsequently annealed at 500°C for 15 minutes. Mcirofabrication was performed using electron beam lithography and Ar ion etching, with positive and negative resists. The processes for microfabrication with positive resist, which were used for most of the dot samples, included: a positive EB resist (ZEP520A) was spin-coated on the thin film and an anti-dot array of the EB resist was patterned. Then, a 10 nm-thick Al-O layer was deposited on the anti-dot array as an etching mask. After lifting off the EB resist, the thin film was etched by Ar ions, and patterned into a well-defined circular shape. Annealing after microfabrication was performed at 500°C for 15 minutes, which was the same annealing condition as that before microfabrication. $L1_0$-FePt (001) particulate films were prepared on MgO (001) substrates using the same sputtering system as that for continuous films. The nominal thickness and the substrate temperature were 25 nm and 630°C, respectively, resulting in the formation of island structure. The measurement methods included X-Ray Diffraction (XRD), Atomic Force Microscopy (AFM), Superconducting Quantum Interference Device (SOUID) magnetometer, Magnetic Force Microscopy (MFM), and Magneto-Optical Kerr Effect (MOKE).

3. Magnetization reversal process in microfabricated $L1_0$-FePt dot arrays

XRD patterns showed the formation of $L1_0$ ordered structure for continuous films. They were perpendicularly magnetized with H_c

of 0.8 kOe. After patterning the continuous films into dots with $d = 0.25$ μm. H_c was enhanced up to 7.5 kOe. After post-annealing, H_c further increased, indicating some damages were recovered. The magnetization behavior of the initial and minor magnetization curves indicated that the magnetization reversal in the FePt dots occurred through the nucleation of reversed domains. When the interdot distance was changed from 0.25 to 1 μm, no obvious effect on H_c was found, indicating that the dipole interaction between dots was negligibly small.

Taking into account the deviation of a real magnet from the ideal situation, the phenomenological analysis modifies H_c from the theoretical limit, and it is given by

$$H_c = \alpha \frac{2K_u}{M_s} - N_{eff} M_s \quad , \qquad (1)$$

where K_u and M_s are uniaxial magnetic anisotropy and saturation magnetization, respectively, and the microstructural parameters α and local effective demagnetizing factor N_{eff} are introduced. α is given by

$$\alpha = \alpha_K \alpha_\psi \quad , \qquad (2)$$

where α_K and α_ψ describe the pinning or nucleation effect of the inhomogeneity of the magnetocrystalline energy and the effect of the misalignment of grains, respectively. In the case of nucleation type magnetization reversal process, α_K^{mic} is approximately given by

$$\alpha_K^{mic} \approx \frac{\delta_B}{\pi r_0} \quad , \qquad (3)$$

where $2r_0$ is the width of planar defects, and δ_B is the domain wall width. The parameter fitting of the temperature dependence of H_c, K_u and M_s to the formula (1) gives α and N_{eff}. Figure 1 shows the plot of $H_c/4\pi M_s$ vs. $K_u/2\pi M_s^2$ for the FePt dots before (open squares) and after (closed squares) annealing. Dotted lines show the least-square fits. The defect region ($2r_0$) was estimated from the slopes of the straight lines to be 26 nm and 18 nm for the FePt dots before and after annealing, respectively. The reduction of the defect regions after annealing was in agreement with the enhancement of H_c for the annealed dots. The values of N_{eff} were obtained from the intercepts to be $4\pi\times(-0.05\pm0.02)$ and $4\pi\times(0.12\pm0.09)$ for the FePt dots before and after annealing, respectively. These values of N_{eff} were quite small compared with those reported for rare-earth transition metal sintered magnets, for example, $N_{eff} = 7.2\pi$ for Nd-Fe-B. The small N_{eff} may originate from good crystallinity of the epitaxial films and/or the small dipolar interaction between dots with the well-defined geometry prepared by microfabrication.

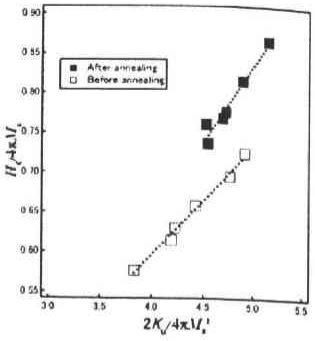

Fig. 1. Plot fo $H_c/4\pi M_s$ vs. $K_u/2\pi M_s^2$ for the FePt dots before (open squares) and after annealing (solid squares). Dotted lines show the least-squares fits.

4. Dot size dependence of magnetization reversal process in microfabricatied $L1_0$-FePt dot arrays

The magnetic properties and the effect of post annealing on magnetic properties of FePt dots with different values of d (0.16, 0.25, 1.0, 2.3, 5.0 μm) were investigated. All the dot arrays showed perpendicular magnetization, and with increasing the dot size, H_c showed a gradual decrease. After post annealing, H_c increased for all the dot sizes except for $d = 0.16$ μm.

The minor loops for different dot sizes were measured and summarized in Fig. 2. H_c and initial magnetic filed (H_{in}) were normalized by H_c^{sat}, where H_c^{sat} corresponded to H_c of the full hysteresis loop. For $d = 0.16$, 0.25 and 1 μm, $H_{in}^{sat}/H_c^{sat} < 1$ showing typical nucleation-type behavior. However, for $d = 2.3$ and 5 μm, $H_{in}^{sat}/H_c^{sat} > 1$, which is possibly caused by the increase of the magnetostatic energy. The phenomenological analysis for $d = 0.25$, 1, 2.3 and 5 μm showed that annealing promoted the recovery from the microfabrication damages, which led to the reduction of $2r_0$ and the enhancement of H_c. $2r_0$ showed a tendency to increase with the dot size, which was consistent with the decrease of H_c. All the dot arrays showed very small N_{eff} compared with those for sintered NdFeB magnets. With changing the dot size, no significant difference for N_{eff} was observed.

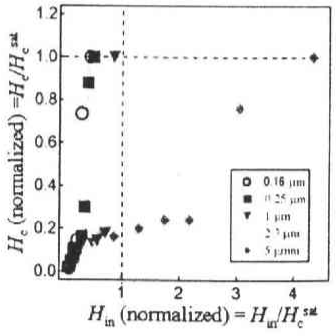

Fig. 2. H_c normalized by the coercivity of the full hysteresis loop (H_c/H_c^{sat}) as a function of H_{in} normalized by the same value of coercivity (H_{in}/H_c^{sat}).

5. Magnetization reversal process in $L1_0$-FePt particulate films

For comparison with FePt dots, FePt particulate films were also investigated. Furthermore, Ar ion irradiation was performed for

particulate films in order to know the effect of structural damages on magnetization reversal process. The phenomenological analysis was applied to FePt particulate films before and after ion irradiation to evaluate $2r_0$ and N_{eff}.

AFM images showed that the FePt particulate films were composed of island-like particles. AFM+MFM revealed that at the thermally demagnetized state, each particle included several magnetic domains. A large H_c = 30.4 kOe was obtained for the FePt particulate film before ion irradiation. After ion irradiation, H_c decreased, which supported the result that microfabrication caused damages. The initial magnetization curves indicated that the magnetization process in the particulate films was a nucleation type before and after ion irradiation.

Table 1. K_u, H_c $2r_0$ and N_{eff} for FePt dots with d = 0.25 μm, FePt particulate films, and sintered NdFeB magnets.

	K_u (×10⁷erg/cc)	H_c (kOe)	$2r_0$ (nm)	N_{eff} (×4π)
FePt dots (d=0.25 μm) (before/after annealing)	2.5 / 3.2	7.5 / 10	26 / 18	-0.05±0.02 / 0.12±0.09
FePt particulate films (before/after ion irradiation)	4.5 / 4.2	30.4 / 21.5	6 /11	1±0.5 / 0.52±0.5
$Nd_{15}Fe_{77}B_8$	4.5	6.5	24	1.8

The results of phenomenological analysis indicated that defect region increased after ion irradiation, which was consistent with the experimental result of the reduction of H_c. The K_u, H_c, $2r_0$, and N_{eff} for FePt dots and FePt particulate films are summarized in table 1. The result reported for NdFeB magnet is also shown for comparison. FePt particulate films show small $2r_0$ and large N_{eff} compared with those of FePt dots, but large $2r_0$ and small N_{eff} compared with those of sintered NdFeB magnets.

6. Mircormagnetic simulation of magnetization reversal process

In order to understand the magnetization reversal process in the FePt dots, micromagnetic simulation was performed for a single FePt dot using public micromagnetic simulator OOMMF (Object Oriented Micromagnetic Framework) based on the Landau-lifshitz equation. Three models, which assumed dots without defects, and with a point-like and planar defect, were chosen to investigate magnetization reversal process in FePt dots. The diameter and the thickness were set at 0.25 μm and 50 nm, respectively, which were the same as those of the experiment.

Figure 3 shows typical simulated results for FePt dots without defects, with a planar and point-like defect. Blue and red regions denote the upward and downward magnetization, respectively. For the dot without defects, the magnetization reversal started at a place between the center and the circumference of the dot, forming a ring-shaped reversed domain. The reversed domain rapidly propagated over the dot and the simulated H_c of 40 kOe was obtained, which was quite larger than the experimental value. For dots with defects, the nucleation of the reversed domain started from the defect region, and then the reversed domain propagated to the center. It revealed that the defects provided nucleation sites for reversed domain, leading to the decrease of H_c. The simulated H_c showed a similar tendency to the experimental results in which H_c decreased with increasing the defect region.

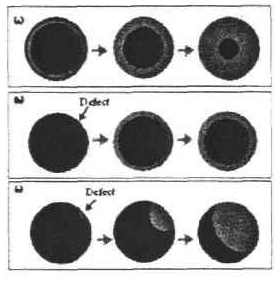

Fig. 3. Time evolution of micromagnetic simulation images for a FePt dot (a) without defects, (b) with a planar defect, and (c) with a point-like defect.

7. Conclusions

Magnetization reversal process in perpendicularly magnetized $L1_0$-FePt (001) dot arrays with different dot sizes was investigated. The initial magnetization processes for dots with d = 0.16, 0.25 and 1 μm showed typical nucleation type behavior. Post-annealing promoted the recovery from the microfabrication damages and led to the improvement of H_c for the dots, which was supported by the result of the phenomenological analysis: $2r_0$ was reduced after annealing.

FePt dot arrays showed large $2r_0$ and small N_{eff} compared with those of the FePt particulate films and the sintered NdFeB magnets. The small N_{eff} may result from the high crystallinity of epitaxial films and/or the small dipolar interaction between dots with well-defined geometry prepared by lithographical technique.

Simulated results for a FePt dot showed that a defect provided a nucleation site for a reversed domain and led to the decrease of H_c, irrespective of the shape and the location of defects.

論文審査結果の要旨

$L1_0$-FePt 規則合金は非常に高い一軸磁気異方性（K_u=7×10^7 erg/cc）を有し、次世代の超高密度磁気記録や微小磁石用の材料として注目されている。このような応用を考えた場合、微小磁性体の磁化反転過程、すなわち保磁力機構を理解することがきわめて重要である。著者は、$L1_0$-FePt(001)薄膜を微細加工することによって、垂直磁化した微小円形ドットの規則配列を作製し、その磁化反転過程を調べた。NdFeB 系焼結磁石の研究で従来用いられてきた現象論的手法を適用し、磁気特性の詳細な解析を行うとともに、マイクロマグネティクスシミュレーションの結果と実験結果を比較することによって、構造欠陥と保磁力との関係を明らかにした。本論文は、この研究成果についてまとめたもので、全編７章からなる。

第１章は序論であり、本研究の背景および目的を述べている。

第２章では、薄膜の作製方法、微細加工法と、構造および磁気特性の評価方法について述べている。

第３章では、ドット径が 0.25 μm の $L1_0$-FePt(001)ドット配列について、アニール前後における構造と磁気特性の評価を行っている。初磁化曲線およびマイナーループの解析から、磁化反転が反転磁区の核生成によって生じていることを明らかにしている。さらに、磁化、保磁力および磁気異方性の温度依存性を用いた現象論的解析手法によって、反転磁区の核生成サイトとなる構造欠陥の大きさを評価している。アニールによって構造欠陥の大きさが減少することを見出し、それが保磁力の増大をもたらしていることを論じている。

第４章では、ドット径をさまざまに変化させた $L1_0$-FePt(001)ドット配列における磁化反転過程について述べている。ドット径が 1 μm 以下では、磁化反転が反転磁区の核生成によって生じていることを明らかにしている。ドット径の増大とともに保磁力は減少し、構造欠陥の大きさは増大する傾向を見出している。また、現象論的解析手法によりドットの有効反磁界係数も評価し、ドット径によらず有効反磁界係数が著しく小さいことを述べている。

第５章では、$L1_0$-FePt(001)ナノ粒子集合体と見なすことができる島状薄膜の磁気特性を調べ、現象論的解析手法により、構造欠陥の大きさと有効反磁界係数を評価している。$L1_0$-FePt(001)ドット配列と比較して、構造欠陥は小さく、有効反磁界係数は大きい傾向があることを明らかにし、保磁力、構造欠陥および有効反磁界係数の３つの関係について論じている。

第６章では、マイクロマグネティクスに基づくモデル計算による磁化反転過程のシミュレーションを行い、実験結果と比較している。適当な構造欠陥を仮定することにより、シミュレーション結果は実験結果とよく一致することを述べている。

第７章は結論である。

以上要するに本論文は、垂直磁化した $L1_0$-FePt(001)ドットの規則配列を作製し、その磁化反転過程を詳細に調べ、構造欠陥と保磁力との関係を明らかにしている。$L1_0$-FePt 規則合金の超高密度磁気記録や微小磁石への応用に向けて重要な知見を与えるもので、材料物性学の発展に寄与するところが少なくない。

よって，本論文は博士(工学)の学位論文として合格と認める。